Electrochemical study of the tarnish layer of silver deposited on glass

Yasser Ben Amor, Eliane Sutter, Hisasi Takenouti, Bernard Tribollet, M. Boinet, R. Faure, J. Balencie, G. Durieu

Electrochemical study of the tarnish layer of silver deposited on glass

Y. Ben Amor[1,2,3,(a)], E. Sutter[1,2,(b)], H. Takenouti[1,2,(b)], B. Tribollet[1,2,(b)], M. Boinet[4], R. Faure[4], J. Balencie[4], G. Durieu[4]

[1] CNRS, UPR 15, Laboratoire Interfaces et Systèmes Electrochimiques, LISE (case courrier 133), 4 Place Jussieu, 75005, Paris, France

[2] UPMC Univ. Paris VI, UPR 15, LISE, 4 Place Jussieu, 75005, Paris, France

[3] Université de Carthage, Institut supérieur des sciences et Technologies de l'environnement de Borj-Cédria B.P 1003, Hammam – Lif 2050, Tunisie

[4] Saint-Gobain Recherche, 39 quai L. Lefranc, BP 135, 93303 Aubervilliers, France

[(a)] Corresponding author: yasser_ben@yahoo.fr, Fax : +33 1 4427 4074

[(b)] ISE member

Abstract

Cyclic voltammetry (CV) and electrochemical impedance spectroscopy (EIS) were used to characterize the tarnished thin layer of silver deposited on glass. Instead of natural tarnishing in air environment, an acceleration of tarnishing process was realized by immersion of Ag covered glass in 10 μM K_2S medium. The X-ray photoelectron spectroscopy (XPS) shows that tarnishing product formed on the silver surface consisted of Ag_2S and Ag_2O. As electrochemical characterization, the measurements were carried out in aerated 0.5 M Na_2SO_4 solution adjusted at pH 10. The impedance spectra collected in sulphate medium at the open-circuit potential show one capacitive loop in parallel with a high resistance, which reflects a blocking electrode behaviour. However, the equivalent electrical circuit, Rs-(CPE//R) is insufficient to reproduce the experimental results correctly. To minimize the dispersion between the experimental and fitted data, the CPE contribution is replaced by two normal power-law distributions of the local resistivity to interpret the tarnishing process in K_2S medium with respect to the immersion time. These distributions are associated with the Ag_2S and Ag_2O layers.

Keywords

Tarnishing process; voltammetry; electrochemical impedance spectroscopy (EIS); normal power-law distribution

1. Introduction

Silver is considered as a noble or semi-noble metal because of its rather high ionization potential. This metal is employed since many centuries for coinage, jewellery, and for making useful or ornamental articles. Its application in industry has increased steeply in recent years. For continuous challenge to improve the durability of products, many research works deal with the ageing mechanism. Such studies are conducted on glass covered with a silver layer submitted to the outdoor aggression where the lifetime is one of the keen issues. The corrosion phenomenon of silver and silver alloy under atmospheric conditions is frequently called tarnishing [1]. The tarnishing process of silver depends on many factors [2-9], such as pH, humidity, temperature, nature and concentrations of pollutants, and exposure time. Moreover, it is often noted that silver and silver compounds have strong interactions with sulphur. Numerous investigators [9-11] have studied the phase transformation from silver to silver sulphide (Ag_2S). The standard redox potential for the overall reaction between Ag and Ag_2S is given by:

$$Ag_2S + 2\ e^- \rightarrow 2\ Ag + S^{2-} \qquad E^0 = -0.691\ V_{SHE} \qquad (1)$$

The standard equilibrium potential E^0 is low, this is the reason that the silver sulphide is readily formed on silver surface.

For more detailed descriptions of the tarnishing process, two mechanisms are often proposed. *Huong* and *Parson* [8] suggest the formation of silver sulphide through the following equation:

$$2\ Ag^+ + SH^- + OH^- \rightarrow Ag_2S_{ads} + H_2O \quad E^0 = -0.390\ V_{SH} \qquad (2)$$

According to this mechanism, an adsorbed silver sulphide layer is formed on the silver surface. It results from reaction between SH^- and Ag^+ ions presumably dissolved at the surface of the silver metal.

The second mechanism was proposed by *Birss* and *Wright* [7]. It consists of two consecutive single electron transfer reactions, as shown by the following equations:

$$Ag + SH^- \rightarrow AgSH_{ads} + e^- \quad (3)$$

$$Ag + AgSH_{ads} + OH^- \rightarrow Ag_2S_{ads} + H_2O + e^- \quad (4)$$

The first reaction, equation (3), relatively fast, leads to the formation of $AgSH_{ads}$ as a surface intermediate. During the second reaction (equation (4)) the intermediate diffuses rapidly on the surface to react with OH^- to form silver sulphide. Besides, a further oxidation of silver or silver sulphide may occur, and leads to the formation of silver oxides such us Ag_2O and AgO [9-11].

To characterize these different tarnish products, several authors [12-16] have used electrochemical methods such as cyclic voltammetry (CV), linear sweep voltammetry (LSV), and square wave voltammetry (SWV). Electrochemical impedance spectroscopy (EIS) has also been applied to study the tarnishing of silver layer and to evaluate the effectiveness of some corrosion inhibitors of metallic silver [17-18]. The EIS measurements have often been analysed by means of equivalent electrical circuit model with two constant phase elements (CPE), which takes into account the diffusion process and the heterogeneity of the working electrode surface [19-20].

In this paper, first, the chemical composition of the tarnish layer was studied by XPS analysis. Then, the electrochemical methods were used to allow the identification and characterization of thin tarnish layers formed on silver immersed during different periods in 10 µM K_2S solution. This solution was used to accelerate the tarnishing process with regard to sulphide polluted atmosphere. The interaction between oxide (Ag_2O) and sulphide (Ag_2S) was discussed. Blank samples have been reduced at -0.7 vs SSE/V during 10 minutes and used as reference. The impedance data collected under different experimental conditions were analyzed by considering two impedances each one being representation of a layer (Ag_2S and

Ag_2O), and different parameters were obtained. These parameters were related to the dielectric properties of the tarnish layers formed on the silver electrode surface.

2. Experimental conditions

2.1. Solutions

Electrolytes were prepared of analytical grade reagents: anhydrous sodium sulphate (Na_2SO_4), sodium hydroxide (NaOH), and potassium sulphide (K_2S). They were dissolved in deionised water. Silver specimens to be tarnished were immersed in a 10 μM K_2S solution (pH adjusted to 10 by addition of a dilute NaOH) for 2 hours to 3 days at room temperature. In our previous paper, devoted to the protection of silver historical artefacts against a tarnishing, 10 mM Na_2S solution was used [17]. However, for the present study, this solution was found to be too aggressive for characterization. This is the reason that the experiments were carried out in a very dilute sulphide medium. The electrolyte used for the characterization of tarnished silver was 0.5 M Na_2SO_4. The pH of which was adjusted also to 10 by addition of a dilute NaOH. The tarnished specimens were quickly transferred to this characterization medium after rinsing the specimen surface with deionised water.

2.2. Electrochemical measurements

Silver was deposited on glass by an electroless industrial process. The thickness of silver layer obtained was about 100 nm. Glass with silver deposit is then cut into 30 × 60 mm coupon for use as the working electrode. The tarnish layers were characterised by electrochemical impedance spectroscopy (EIS) using a Gamry G300 instrument. The impedance was recorded, after 30 min of stabilization at the open circuit potential, by applying a 10 mV_{rms} perturbation and sweeping frequency from 100 kHz to 10 mHz with 10 points per decade. The measurements were carried out in a three electrodes cylindrical cell (Fig. 1). The working electrode area (1.8 cm^2) was limited by a silicon O-ring. A Cu wire ensures the electrical

contact with the potentiostat. A saturated sulphate electrode (SSE) and a large platinum plate were used for reference and counter electrodes, respectively. To minimize the artefacts sometimes observed at high frequency domain (HF) due to high impedance of the reference electrode, the latter was coupled with a platinum wire through a capacitor of 0.47 μF [21].

3. Results and discussion

3.1. Composition of the tarnishing layer

To determine the composition of the tarnishing layer, XPS analysis, cyclic voltammetry, and EIS measurements were performed on the reference (cathodically reduced silver) and tarnished electrodes.

3.1.1. XPS analysis

The characterization of the tarnish layer was realized by XPS for ca. 5 nm depth. The recorded spectra show the presence of peaks characteristic of C-H bonds related to the contamination of the samples. The element S is present as soon as the sample was immersed in the tarnishing medium. The energy level of S2p at 161 eV is compatible with the presence of an Ag_2S layer at the top. Auger spectra identified the presence of Ag_2O at the upper surface layer on the reference sample and before tarnishing. During the tarnishing process, Ag_2S covers progressively the Ag_2O layer.

3.1.2. Cyclic voltammetric responses without tarnishing

Two cyclic voltammograms of the working electrode without tarnish layer, and immersed in 0.5 M Na_2SO_4 are presented in Fig. 2. The potentials were referred to the standard hydrogen electrode (SHE) by adding 0.651 V to the experimental potential. The voltammogram with solid line curve was recorded after cathodic reduction at -0.05 vs SHE/V during 10 minutes to reduce a tarnish layer eventually formed during the electrode storage. The dotted curve was directly recorded without cathodic conditioning of the working electrode. In both cases, the

potential scanning was performed from the initial potential E_i close to the open circuit E_{oc}, then scanned in the cathodic direction, from the open circuit potential (ca. 0.4 vs SHE/V) to -1.245 vs SHE/V and then to anodic potential up to 2.245 vs SHE/V. The scan rate was 5 mV s^{-1}. Fig. 2a shows the whole current range, whereas Fig. 2b displays the cathodic current in the enlarged scale. The two curves show qualitatively the same shape.

The cathodic voltammograms exhibit the presence of a current plateau at -20 µA cm^{-2} corresponding to the reduction of dissolved oxygen. A peak with a low intensity at -0.05 vs SHE/V, which disappears during the anodic scan, can be observed. The origin of this peak is not clear. Some authors [23] have observed the same peak in alkaline media before the reduction of dissolved oxygen. They attributed this electrochemical behaviour to the reduction of oxygenated species of Ag(I). However, other authors [24] have not observed this peak on silver electrodes that were initially reduced at cathodic potential. Furthermore, a cathodic peak preceding the reduction of dissolved oxygen was also observed with stainless steel in aerated solution of Na_2SO_4 and natural water. This peak was attributed to the reduction of oxygen and some residual oxide layers formed in air before immersion [25].

The charge involved at peak C_1 was evaluated by integration. Table 1 summarizes the results. From the compact atomic arrangement of Ag for an ideally flat electrode, the charge was transformed into the number of monolayers. 4 to 5 mono-layers were estimated which correspond to a thin layer, but significantly greater than sub-molecular adsorbed O or OH at the silver surface.

A small current peak observed for the silver specimen without cathodic reduction at about 0.9 vs SHE/V may corresponds the reduction of residual tarnish layer formed during the storage of the silver-deposited glass in desiccator.

During the anodic scan (Fig. 2a), an anodic peak (A) situated at 0.8 vs SHE/V was observed and attributed to the oxidation of Ag_2O to AgO according to the following equation [22]:

$$Ag_2O + 2\ OH^- \rightarrow Ag_2O_2 + H_2O + 2e^- \quad E^0 = 0.607\ V_{SHE} \qquad (5)$$

It is worth to recall that the equilibrium potential of this reaction in pH 10 medium is ca. 0.85 vs SHE/V.

The formation of Ag_2O preceding this peak was not clearly observed, therefore the peak A may involve also a direct formation of Ag to AgO.

3.1.3. Cyclic voltammograms of the tarnished silver samples

The cyclic voltammetric curves of tarnished electrodes exhibited the same shape whatever the tarnishing period. Fig. 3a presents the voltammograms recorded for 2, 24, and 78 h tarnishing time in 10 μM K_2S. Fig. 3b shows the same voltammograms but enlarged current scale to illustrate more clearly various cathodic peaks.

The voltammograms (cf. Fig. 3b) did not show clearly a reduction peak C_1, but around -0.52 vs SHE/V the second peak C_2 is observed. Fig. 3c presents the voltammograms with enlarged potential and current scale. The tarnish layer is thus likely reduced at this current peak. The equilibrium redox potential of this reaction at pH 10 solution was calculated as -0.69 vs SHE/V, slightly more negative than peak potential C_2. Its intensity increases with the tarnishing time. The charge and the corresponding number of molecular layers below this peak are indicated in Table 2. The amount of Ag_2S reduced at this peak is therefore significantly smaller than that evaluated by XPS analyses. Only a small part of the tarnish layer is likely to be reduced at this peak potential. Beyond this peak a plateau between -0.65 vs SHE/V and -0.8 vs SHE/V appears. It was assigned to the reduction of dissolved oxygen as in case of the reference silver electrodes. An increase in the cathodic current is then observed beyond -1.5 vs SHE/V. It corresponds to the reduction of water with hydrogen evolution reaction. An additional peak was observed at ca. -1.2 vs SHE/V before the hydrogen evolution reaction. This peak may be allocated to the reduction of remaining Ag_2S layer by the following reaction:

$$Ag_2S + 2\ H^+ + 2\ e^- \rightarrow 2\ Ag + H_2S \qquad E_{eq} = -1.2\ V_{SHE} \text{ at pH } 10 \qquad (6)$$

The peak height is about 10 times grater than C_2 peak, thus with these two peaks, the amount of Ag_2S accumulated on the silver surface during the immersion in 10 µM K_2S becomes close to those estimated by XPS measurements. It is important to note that the amount of Ag_2S increases with immersion period.

During the anodic scan, the peak at around 0.8 vs SHE/V was observed. However, a careful observation of this peak showed in fact three anodic peaks, A_1(0.62 vs SHE/V), A_2 (0.73 vs SHE/V) and A_3 (0.80 vs SHE/V) as could be seen in Fig. 3d. The peak current densities A_1 and A_2 increase with immersion period whereas the peak height of A_3 decreases. Moreover, it can be noted that the potential of this peak was slightly shifted to less anodic values when the tarnishing time increases.

Since A_3 has a potential close to that observed for reference electrode (peak A), it is allocated to the same reaction. Peak A_2 was attributed to the oxidation of the Ag to Ag_2O according to the following equation [26]:

$$2\ Ag + 2\ OH^- \rightarrow Ag_2O + H_2O + 2e^- \qquad E_{eq} = 0.58\ V_{SHE} \text{ at pH } 10 \qquad (7)$$

The origin of Peak A_1 is difficult to identify, but may be associated with the formation of $AgSO_4$ according to the following reaction:

$$Ag_2SO_4 + 2\ e^- \rightarrow 2\ Ag + SO_4^{2-} \qquad E_{eq} = 0.62\ V_{SHE} \text{ at } [SO_4^{2-}] = 0.5\ M \qquad (8)$$

It is worth to emphasize that these peaks are not directly related to the tarnish layer, since they are reduced during the cathodic scan, and the electrolyte used for this measurement does not contains sulphide ions. The difference observed for the anodic peak with respect to the immersion period in tarnishing solution is thus likely to be due to the surface roughness.

3.2. Electrochemical impedance

Electrochemical impedance spectroscopy investigations of tarnished silver were performed at open circuit potential (*OCP*) after 30 min of stabilization in 0.5 M Na_2SO_4 adjusted at pH 10. Fig. 4 shows the impedance diagrams in both Nyquist and Bode plots for reference (only Ag_2O layer) and tarnished samples for 2 h and 78 h. All impedance spectra in Nyquist plot (Fig. 4a) were characterized by one capacitive loop with a high resistance in parallel. The diameter of this loop is greater for the tarnished samples. Fig. 4b shows the corresponding Bode plot. It can be noted also that no significant change of the impedance was observed beyond 4 h immersion. At the same time, at low frequencies, the phase is higher for tarnished sample. This behaviour is probably related to the Ag_2S layer, which covers the metallic electrode and the oxide layer.

To evaluate the electrochemical behaviour obtained by impedance measurements, in a first approach an equivalent circuit was adopted to reproduce the experimental results (Fig. 5a). In this circuit, R_s is the solution resistance, R is the resistance of the tarnish and oxides layers in parallel to a *CPE* related to the blocking nature for these layers. To assess the agreement between the experimental (Z_{exp}) and the fitted data (Z_{fit}), the error on imaginary component was calculated according to the following equation:

$$\varepsilon_{Z(im)} = 100 \frac{Z_{\exp}(im) - Z_{fit}(im)}{Z_{\exp}(im)} \qquad (9)$$

Fig. 6 shows the presence of systematic and marked divergences on the imaginary part of the impedance ($Z(im)$) mainly above 100 Hz (curve with solid line). Therefore, another impedance model must be used to correctly reproduce the experimental impedance data.

3.2.1. Power-law model for normal resistivity distribution

One of the manners to characterize a CPE behaviour is the representation by a distribution of the resistivity of the films in the normal direction to the electrode surface [27-28]. The film resistivity was written as [27]:

$$\frac{\rho_\xi}{\rho_\delta} = \left[\frac{\rho_\delta}{\rho_0} + \left(1 - \frac{\rho_\delta}{\rho_0}\right) \xi^\gamma \right]^{-1} \tag{10}$$

where ρ_0 and ρ_δ are the boundary values of resistivity at the interfaces, $\xi = x/\delta$ (x is the distance along the film thickness) and γ is a parameter indicating how sharply the resistivity varies.

This approach assumes that the dielectric constant of the film is independent of the position. Under this assumption, an impedance response showing *CPE* behaviour can be explained in terms of a power-law distribution of resistivity. This impedance can be expressed as [27]:

$$Z_{\mathrm{pl}}(\omega) = g \frac{\delta \cdot (\rho_\delta)^{1/\gamma}}{\left(\frac{1}{\rho_0} + \mathrm{j} \cdot \omega \cdot \varepsilon \cdot \varepsilon_0 \right)^{(\gamma-1)/\gamma}} \tag{11}$$

In this equation, j and ω represent respectively the imaginary number $\sqrt{-1}$ and the angular frequency ($2\pi f$ with f in Hz), ε_0 is the vacuum permittivity (9. 10^{-14} F cm^{-1}) and ε is the relative permittivity of the film. The function g was evaluated digitally and can be expressed as a function of γ only [27]:

$$g = 1 + 2.88 \cdot \gamma^{-2.375} \tag{12}$$

(γ-1)/1 can be replaced by α according to:

$$\alpha = \frac{\gamma - 1}{\gamma} \tag{13}$$

This α is identified as the *CPE* coefficient.

When $(\rho_0 \cdot \varepsilon \cdot \varepsilon_0)^{-1} < \omega < (\rho_\delta \cdot \varepsilon \cdot \varepsilon_0)^{-1}$, the equation (10) can be expressed as:

$$Q = \frac{(\varepsilon \cdot \varepsilon_0)^{\alpha}}{g \cdot \delta \cdot \rho_\delta^{1-\alpha}} \tag{14}$$

It can be noted that equation (14) is used to relate the *CPE* parameters to the physical properties of the film. Hirschorn et al. [29] have used this model to characterise various systems such as aluminium oxides and oxides on stainless steel. They obtained good values of the thickness of different studied layers.

Equation (11) was applied, first, to reproduce the impedance data recorded on a reference sample without tarnishing (reference curve in Fig. 4). The resistivity ρ_δ of Ag_2O is fixed to 450 Ω cm. This value was proposed by Hirschorn et al. [27] to reproduce the impedance data of oxide formed on Fe17Cr stainless steel disk in 0.05 M Na_2SO_4 at pH 4. The values of the relative permittivity ε of Ag_2O is fixed to 8.8 [30]. The knowledge of these values allows the characterization of the Ag_2O layer by the coefficient γ, the resistivity ρ_0, and the layer thickness δ. These parameters were evaluated by a non-linear regression method based on a simplex procedure with a house made software by using the expression of equation (11). The results of these variables are summarized in Table 3. The error margin was evaluated from five replica measurements.

Then, the experimental impedance spectra on tarnished samples were represented by the equivalent circuit presented in Fig. 5b. This circuit takes into account the contribution of two layers, Ag_2S and Ag_2O, formed upon the metallic silver layer in agreement with XPS analyses. In this circuit, each layer is represented by a normal distribution of *RC* elements (Fig. 5c) Integrating this distribution leads to the expression of equation (11). The total impedance is expressed as:

$$Z_{\text{exp}}(\omega) = R_s + Z_{\text{pl}}(\text{Ag}_2\text{S}) + Z_{\text{pl}}(\text{Ag}_2\text{O}) \tag{15}$$

Where Z_{pl} is given by equation (11)

The permittivity ε and the resistivity ρ_δ of Ag_2S are fixed to 3.5 and 400 Ω cm respectively [30]. The same calculation procedure was applied to determine the characteristic parameters of each layer. The corresponding error (Equation 8) was presented in Fig. 6 (curve with dot line). It was clearly seen that the proposed model no longer induces a systematic error.

3.2.2. Results various parameters obtained by regression calculation

The variation of the different parameters of the adopted equivalent circuit (Fig. 5b) with respect to the tarnishing period was presented in Fig. 7. All parameters, except the coefficient $\gamma(Ag_2O)$, vary scarcely with the K_2S immersion time. This result indicates that 2 h of immersion in 10 µM K_2S medium seems to be sufficient to achieve the steady state values of the tarnish layer. The coefficient $\gamma(Ag_2O)$ (Fig. 7a) decreased from 24.4 to 13.5 when the tarnishing time increases from 2 h to 78 h. These values are slightly higher than that determined with the reference sample ($\gamma(Ag_2O)=10.2 \pm 1.2$). However, the value of the corresponding *CPE* exponent α, determined from equation (13), remain above 0.9. Fig. 7a shows also that $\gamma(Ag_2S)$ is substantially constant with the tarnishing time and much lower than $\gamma(Ag_2O)$, with an average value about 2.9. The low value of $\gamma(Ag_2S)$, thus low α value (cf. Eq (13)), suggests that the Ag_2S layer is relatively heterogeneous. The relative resistivity ρ_0 of Ag_2S and Ag_2O layers were presented in Fig. 7b. It can be noted also that the resistivity of Ag_2O formed on both reference and tarnished samples present the same magnitude. The corresponding resistivity profiles calculated from equation (10) are presented in Fig. 7c. These curves illustrate the power-law nature of the distribution. The estimated thickness of each layer is presented in Fig. 7d. The Ag_2S layer thickness is about 4.6 nm, more important than that estimated from C_2 peak in voltammograms (Table 2) but close to that estimated from XPS data. In contrast, the thickness of the oxide layer (Ag_2O) is much lower (Fig. 7d). An

average value is estimated to 0.5 nm, close to the monomolecular thickness (0.38 nm for Ag_2O crystal). In the presence of the tarnish layer, the Ag_2O layer becomes thinner. Its estimated thickness on the reference sample is three times higher. The calculated value is about 1.4 ± 0.2 nm (Table 3). Besides, the ratio of Q values (equation 14) corresponding to the Ag_2O layers formed on the surface of reference and tarnished silver is about 3. These values suggest that during the tarnishing process Ag_2O is partially converted into Ag_2S. The Ag_2S may be also formed from the substrate Ag.

4. Conclusions

This work was focused on the characterization of tarnish layer formed on a thin silver deposit on glass substrate. The tarnishing process was induced by immersion in 10 μM K_2S medium adjusted at pH 10. The composition and the nature of the tarnish products were identified by XPS analysis, and cyclic voltammetry is in agreement with this surface analyses. It was shown that sulphide layer (Ag_2S) covers progressively the Ag_2O layer during immersion test. The tarnish layer was then examined in more detail by EIS investigations. Impedance spectra recorded on the tarnished samples show the presence of two impedances. Under the assumption of the uniform dielectric constant for the two layers (independent of the position), two normal power-law distributions of the local resistivity of each layer are consistent with the *CPE* contributions. The good agreement between the experimental data and the equivalent circuit model used allowed validating the model with the values of the different parameters, which have a physical meaning with respect to tarnishing time.

References

[1] T.E. Graedel, J. Electrochem. Soc 139 7 (1992) 1963.

[2] D.W. Hatchett, X. Gao, S.W. Carton, H.S. White, J. Phys. Chem 100 (1995) 333.

[3] I.C. Hamilton, R. Woods, J. App. Electrochem 13 (1983) 783.

[4] M. Hepel, S. Bruckenstein, G.C. Tanh, J. Electroanal. Chem 261 (1989) 389.

[5] G. Horanyi, G. Vertes, Electrochim. Acta 31 12 (1986) 1663.

[6] D.W. Price, G.W. Warren, B. Drouven, J. Appl. Electrochem 16 (1986) 719.

[7] V. Birss, G.A. Wright, Electrochim. Acta 27 1 (1986) 7

[8] C.N.V. Huong, R. Parsons, J. Electroanal. Chem 119 (1981) 137.

[9] J.I. Lee, S. M. Howard, J.J. Kellar, W. Cross, K.N. Han, Metallurgical and materials transactions B, 32B (2001) 895.

[10] J. Horvath, L. Hackl, Corr. Sci 5 (1965) 525.

[11] S.M. Raghy, M.F. El-Demerdash, J. Electochem. Soc 136 12 (1989) 3647.

[12] A. Doménech-Carbó, J. Solid State Electochem 14 (2010) 363.

[13] V. Costa, K. Leyssens, N. Richard, F. Scholz, J. Solid State Electrochem 14 (2010) 449.

[14] C. Degrigny, J. Solid State Electrochem 14 (2010) 353.

[15] A. Doménech, M. T. Doménech-Carbó, M.A. Peiró, Anal Chem 83 (2011) 5639.

[16] A. Doménech, M.T. Doménech-Carbó, I. Martínez-Lázaro, Anal. Chim. Acta 680 (2010) 1.

[17] M.C. Bernard, E. Dauvergne, M. Evesque, M. Keddam, H. Takenouti, Corr. Sci 47 (2005) 663.

[18] L. Paussa, L. Guzman, E. Marin, N. Isomaki, L. Fedrizzi, Surf. Coat. Tech 206 (2011) 976.

[19] E. Angelini, S. Grassini, M. Parvis, Corrosion Eng. Sci. Tech 45 5 (2010) 334.

[20] M.L. Varsanyi, M. Furko, T. Pozman, Electrochim Acta 56 (2011) 7787.

[21] A.T. Tran, F. Huet, K. Ngo P. Rousseau, Electrochim. Acta 56 (2011) 8034.

[22] N. Li, A. Galtayries, I. Frateur, V. Maurice, European Corrosion congress, Moscow, Russia 1-4 (2010) 406.

[23] S.S. Abd El Rehim, H.H. Hassan, M.A.M. Ibrahim. M.A. Amin, Monatshefte fur Chemie 129 11 (1998) 1103.

[24] J.M.M. Droog, F. Huisman, J. of Electroanal. Chem 115 (1980) 211.

[25] C. Marconnet, Thesis, Electrochimie-Biocorrosion, Ecole centrale de Paris (2007).

[26] S. Capelo, P.M. Homem, J. Cavalheiro, I.T.E. Fonseca, J. Solid State Electrochem 17 (2013) 223.

[27] B. Hirschorn, M.E. Orazem, B. Tribollet, V. Vivier, I. Frateur, M. Musiani, J. Electrochem. Soc 157 12 (2010) C452.

[28] M. Musiani, M. E. Orazem, N. Pébère, B. Tribollet, V. Vivier, J. Electrochem. Soc 158 12 (2011) C424.

[29] B. Hirschorn, M.E. Orazem, B. Tribollet, V. Vivier, I. Frateur, M. Musiani, J. Electrochem Soc 157 12 (2010) C458-C463.

[30] P. Junod, Helvetica Physica Acta, 32 (1959) Fasciculus 6/7.

Table 1: Quantity of electricity involved below the cathodic peak C_1

Cathodic reduction	C_1 (μA s cm^{-2})	Molecular layers
Without	694	4.42
With	850	5.41

Table 2: Quantity of electricity involved below the anodic peak

Immersion period (h)	C_2 (μA s cm^{-2})	Molecular layers	A_1 (mA s cm^{-2})	Molecular layers
2	-53.0	0.346	68.0	442
24	-137	0.890	51.8	336
78	-276	1.792	63.3	411

Table 3: Values of Ag_2O parameters calculated from equation (11)

γ	ρ_0 (Ω cm)	δ (nm)
10.2 ± 1.2	$8.7\ 10^{13} \pm 1.7\ 10^{13}$	1.4 ± 0.2

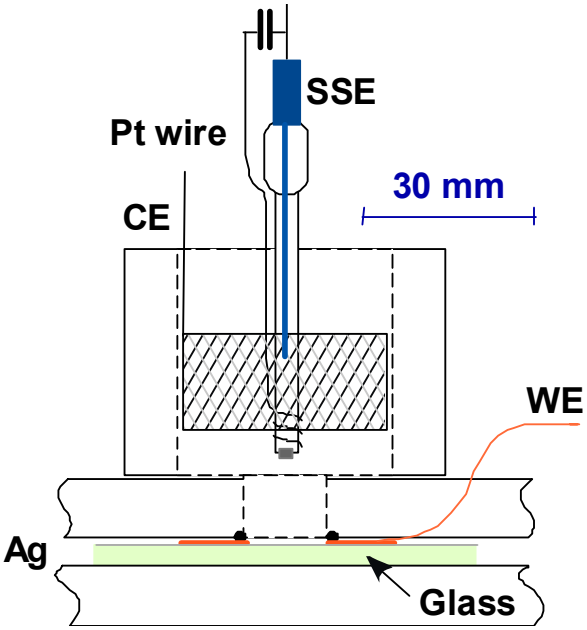

Fig. 1: Electrochemical cell

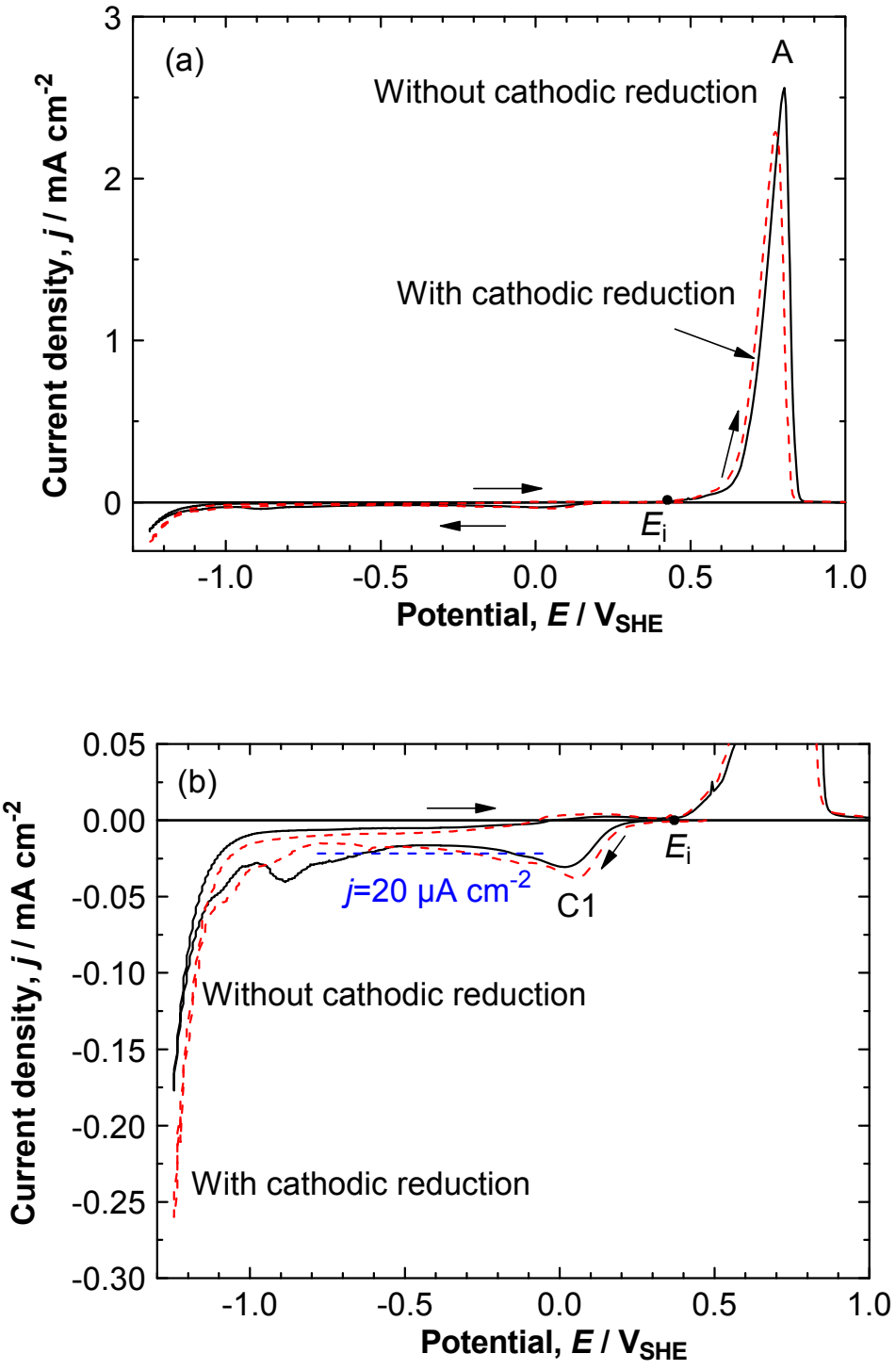

Fig. 2: Cyclic voltammograms of reference silver electrode in 0.5 M Na_2SO_4 (pH = 10). Scan rate: 5 mV s^{-1}, (a) overall plot (b) cathodic domain with enlarged current scale

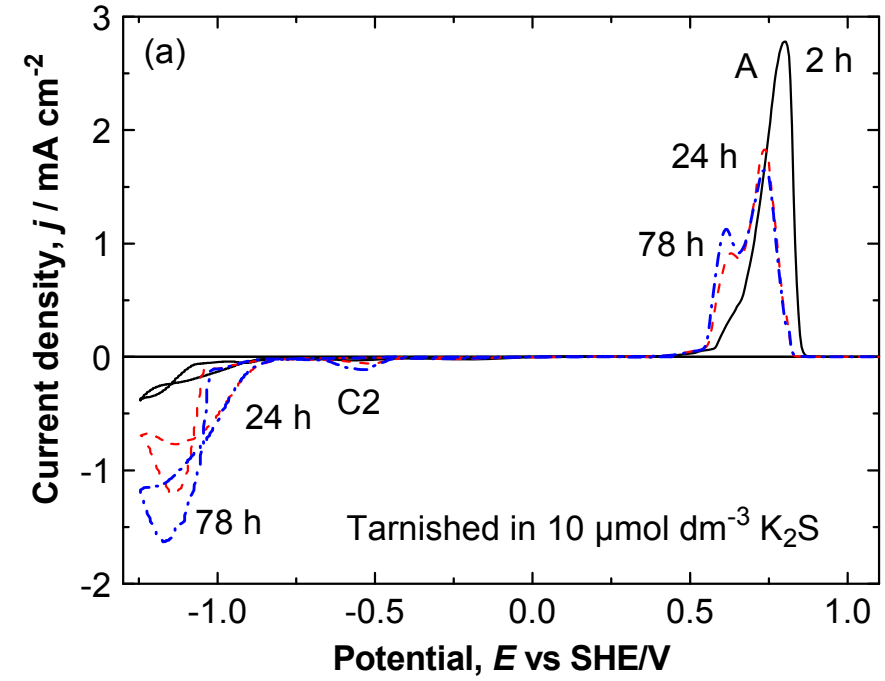
(a)
A
2 h
24 h
78 h
24 h
C2
78 h
Tarnished in 10 μmol dm^{-3} K_2S
Current density, j / mA cm^{-2}
Potential, E vs SHE/V
3
2
1
0
-1
-2
-1.0
-0.5
0.0
0.5
1.0

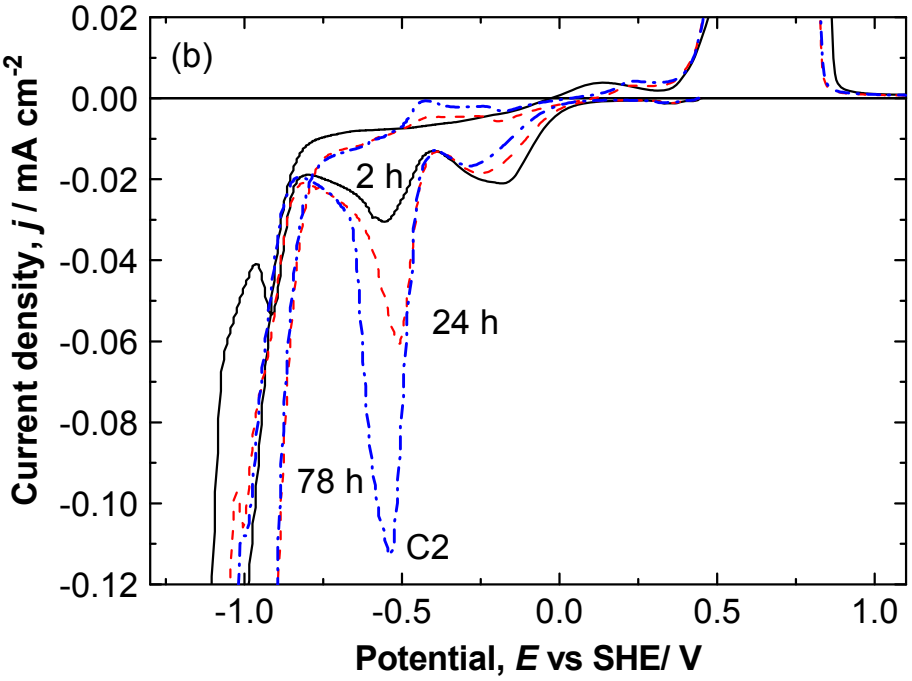
(b)
2 h
24 h
78 h
C2
Current density, j / mA cm^{-2}
Potential, E vs SHE/ V
0.02
0.00
-0.02
-0.04
-0.06
-0.08
-0.10
-0.12
-1.0
-0.5
0.0
0.5
1.0

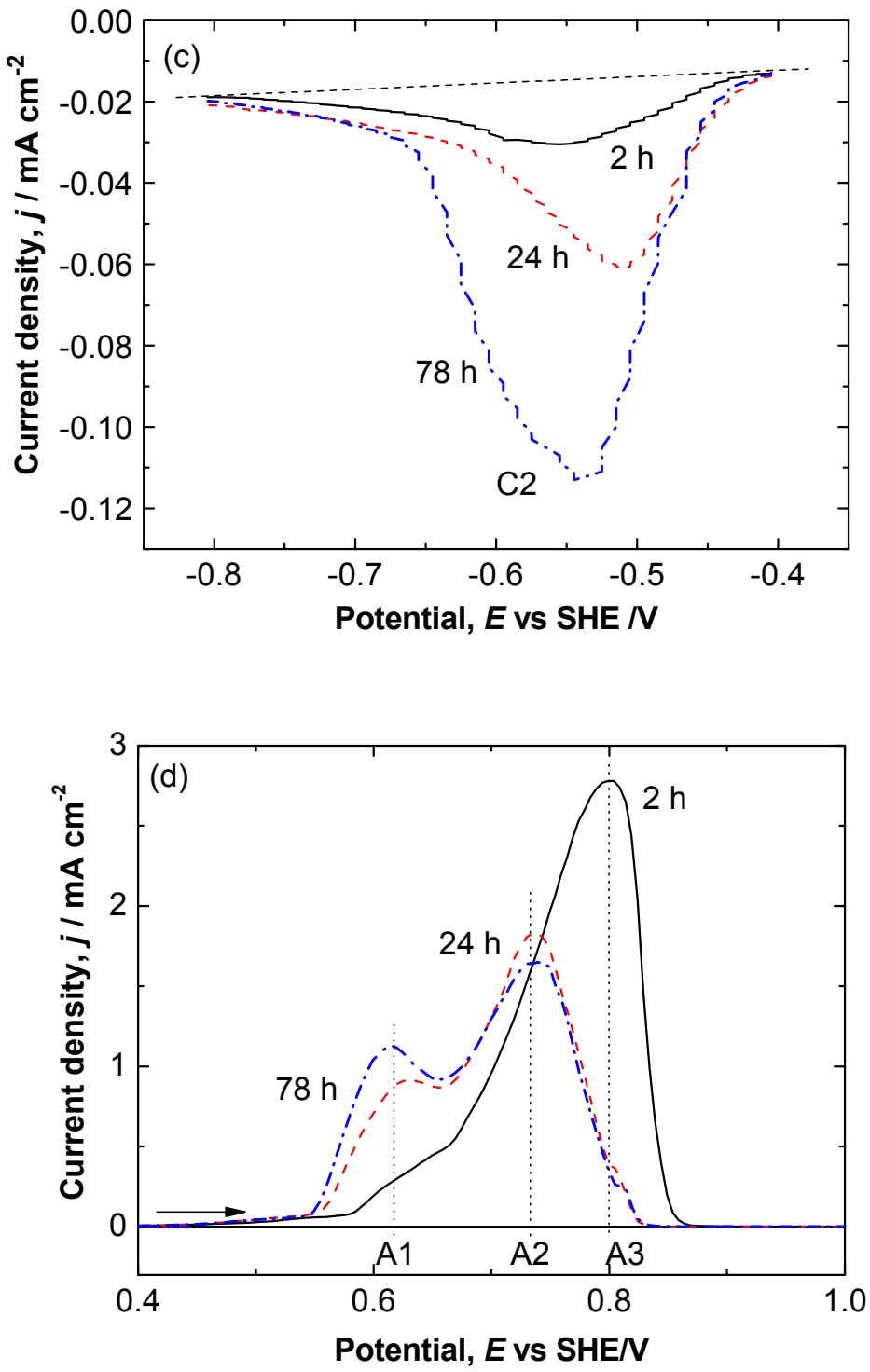

Fig. 3: Cyclic voltammograms of tarnished silver electrodes in 0.5 M Na_2SO_4 (pH = 10). Effect of the tarnishing time. Scan rate: 5 mV s^{-1}: (a) whole current domain, (b) Cathodic current in enlarged scale, (c) cathodic peak C_2 and (d) anodic peaks A_1, A_2 and A_3.

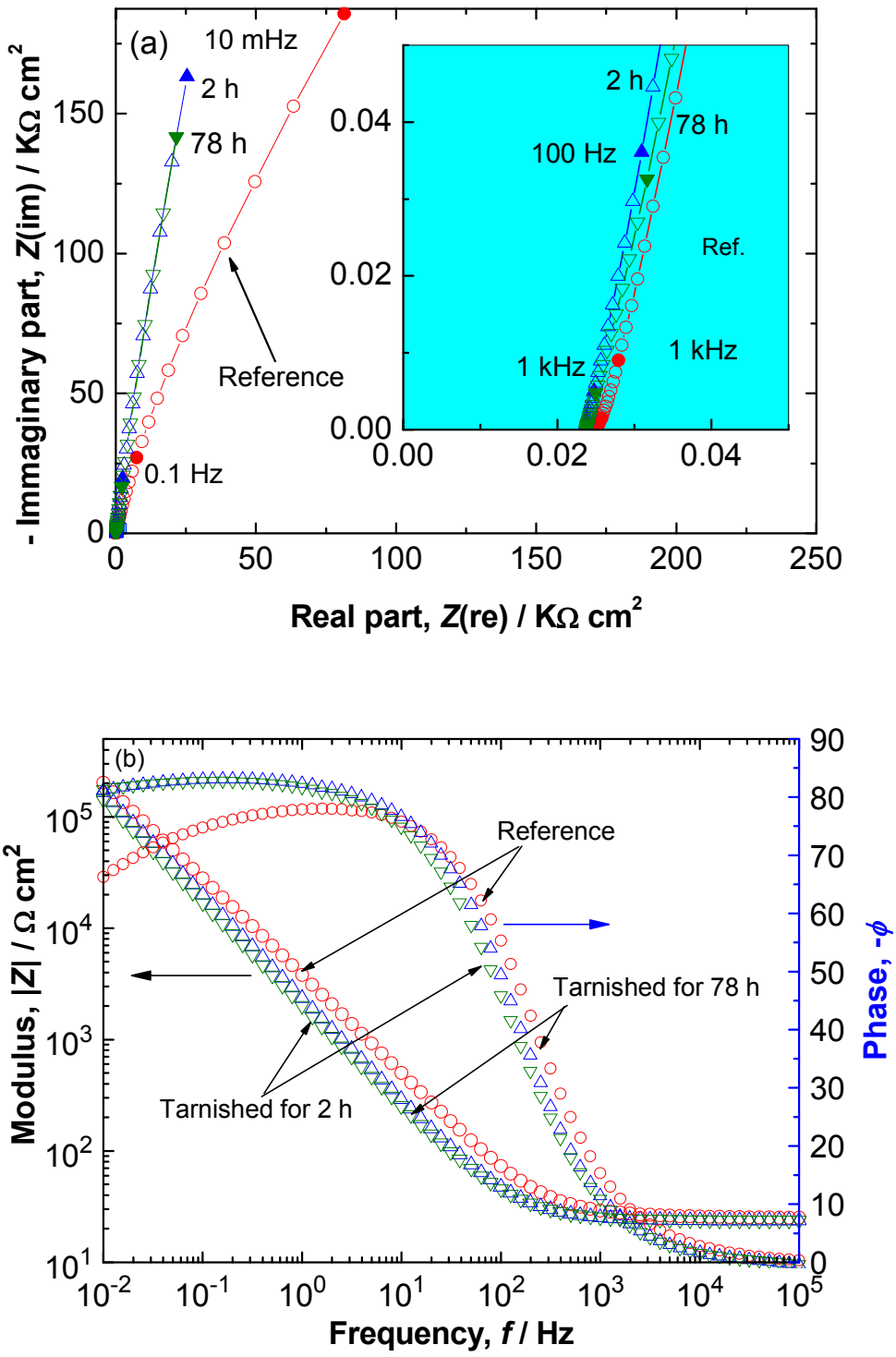

Fig. 4: Impedance diagrams plotted at open circuit potential in 0.5 M Na_2SO_4 (pH = 10)

(a) Nyquist and (b) Bode plot.

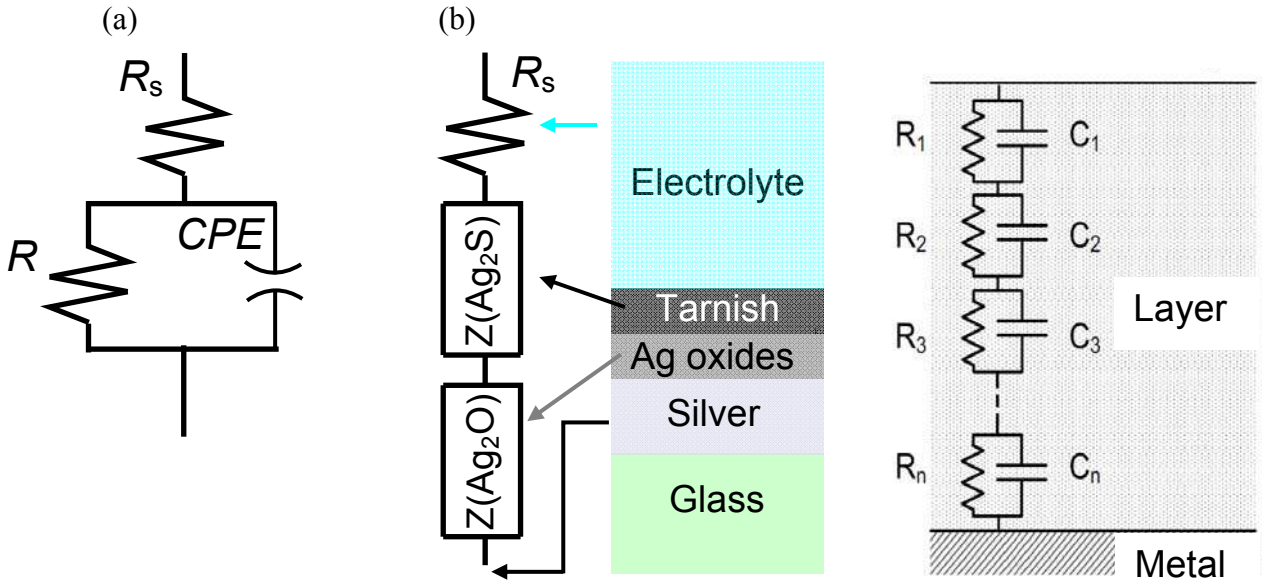

Fig. 5: Equivalent electric circuits used to simulate the impedance spectra of the silver electrode: (a) *CPE* behaviour, (b) Physical attribution of each component of the equivalent circuit, (c) The distribution of RC elements that correspond to the impedance response of each layer.

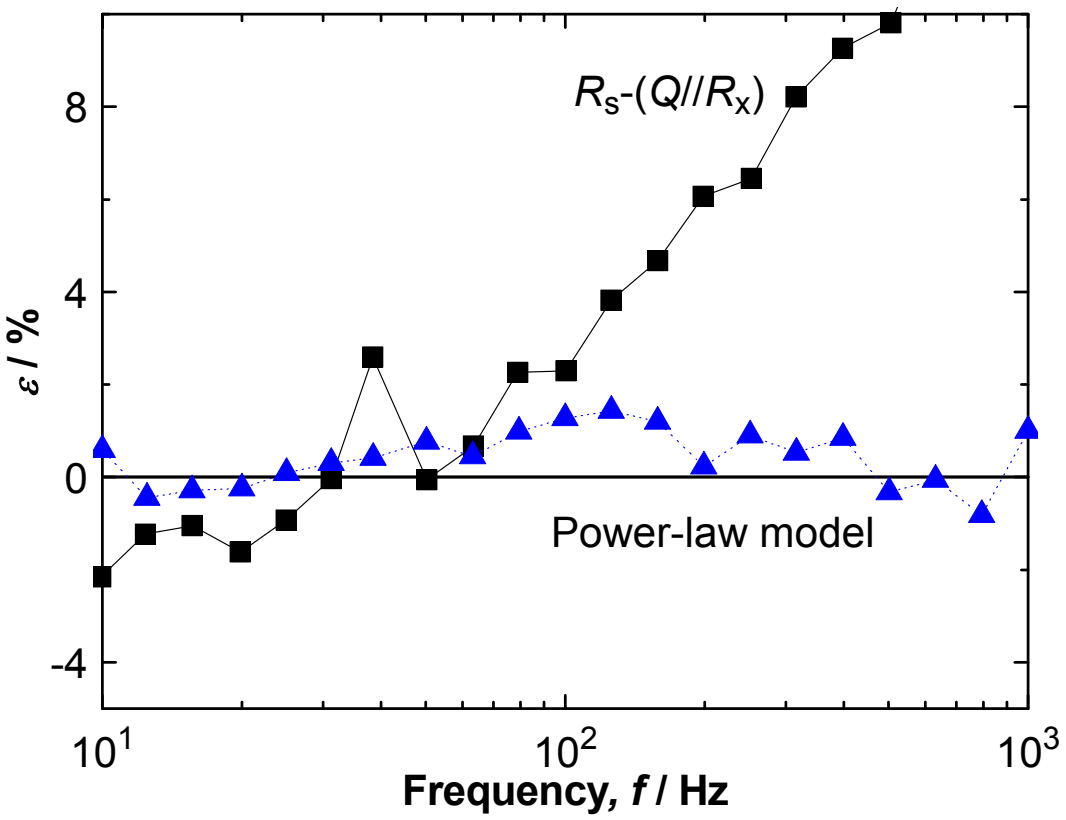

Fig. 6: Variation of the error (6) as a function of frequency. Measurements recorded on electrode silver tarnished for 78 h.

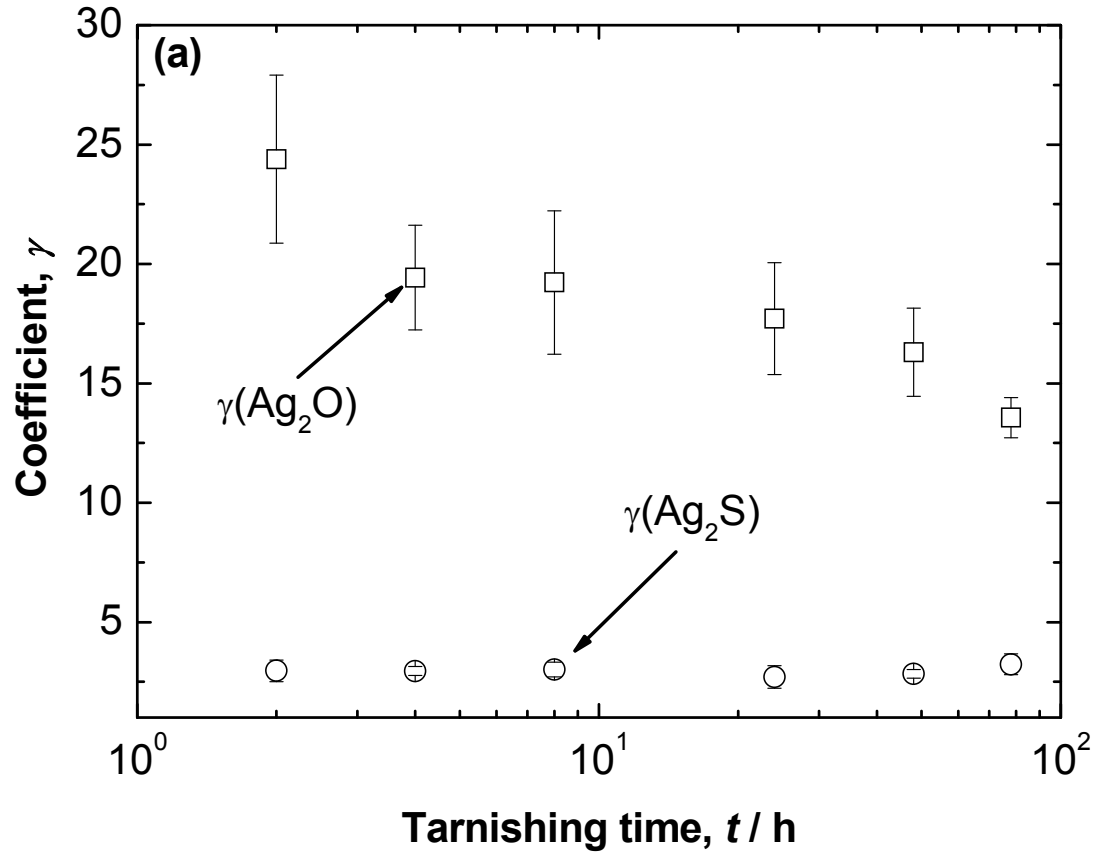
(a)
Coefficient, γ
γ(Ag2O)
γ(Ag2S)
Tarnishing time, t / h

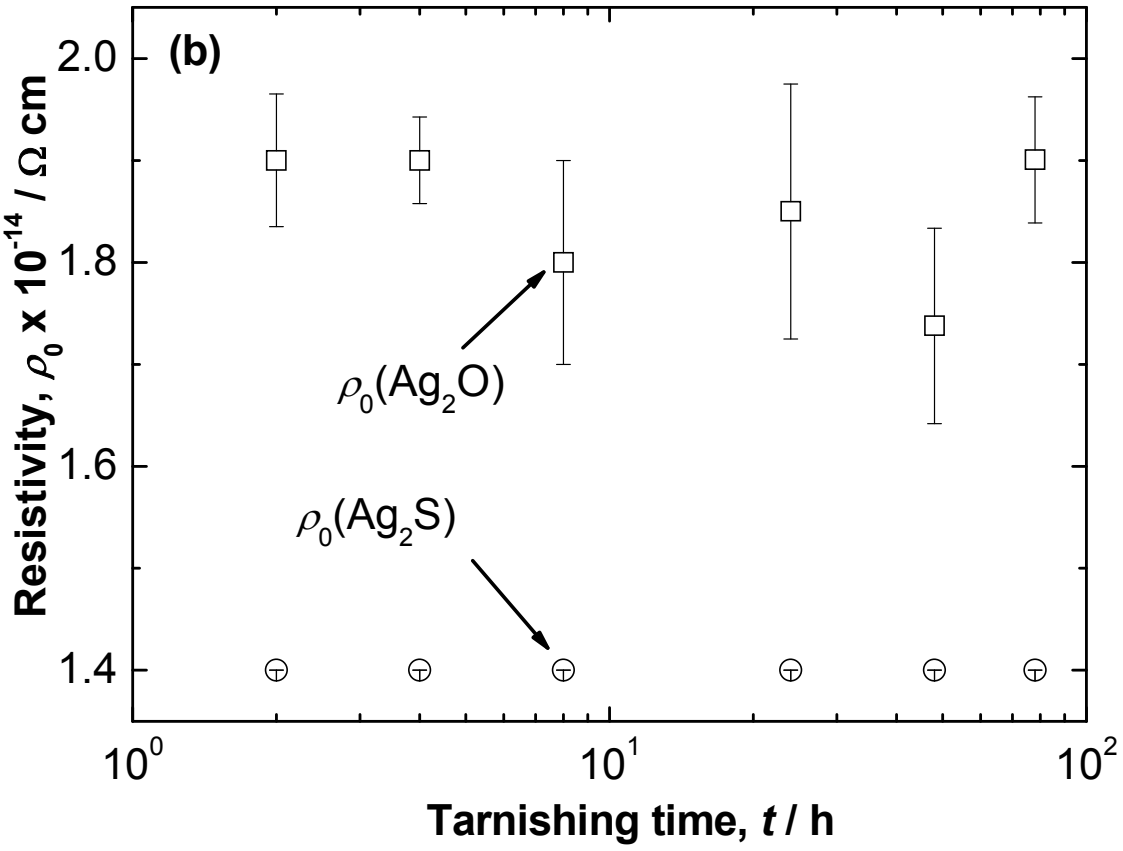
(b)
Resistivity, ρ0 x 10-14 / Ω cm
ρ0(Ag2O)
ρ0(Ag2S)
Tarnishing time, t / h

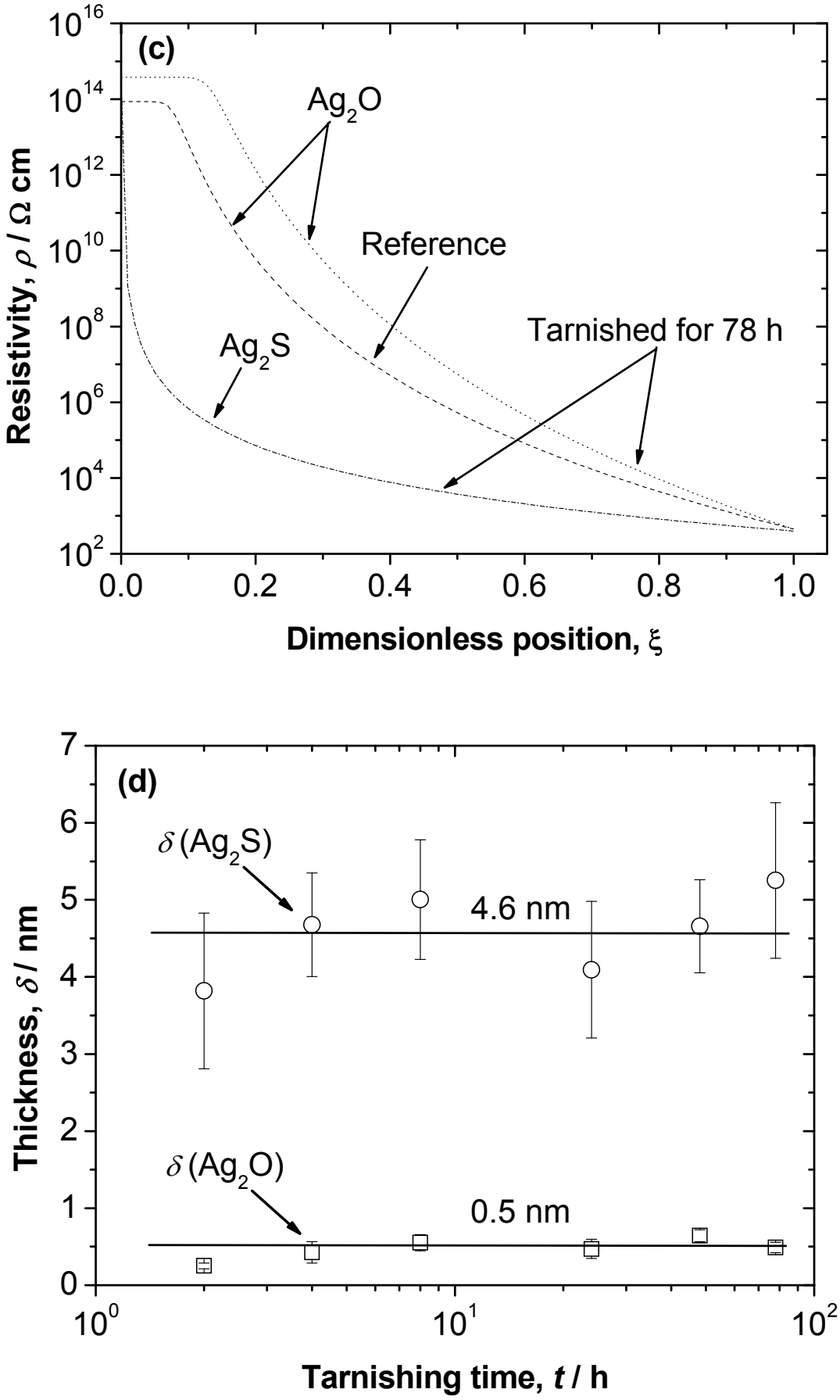

Fig. 7: Variation of the fitting parameters calculated from equations (10), (11), and (15).